**DOI: https://doi.org/10.15276/aait.09.2026.33**
**UDC 004.932:004.94:796.352**

# Markerless video-based golf-stick motion analysis using Kalman filtering and Rauch-Tung-Striebel smoothing

**Ivan M. Syniuk**[1)]
ORCID: https://orcid.org/0009-0000-4141-0135; i.syniuk@gmail.com
**Maksym V. Maksymov**[1)]
ORCID: https://orcid.org/0000-0002-7536-2570; prof.maksimov@gmail.com. Scopus Author ID: 7005088554
**Oleksii M. Maksymov**[1)]
ORCID: https://orcid.org/0000-0003-2504-0853; oleksii.maksymov@op.edu.ua. Scopus Author ID: 57220057510
**Karthik Iyer**[2)]
ORCID: https://orcid.org/0009-0003-2520-1810; ki2406@columbia.edu
[1)] Odesa Polytechnic National University, 1, Shevchenko Ave. Odesa, 65044, Ukraine
[2)] Columbia University, 116th and Broadway. New York, 10027, USA

## ABSTRACT

**Relevance.** Quantitative assessment of golf-stick motion matters for sport biomechanics, coaching, rehabilitation, and virtual-reality training. Laboratory marker-based capture is precise but impractical for routine field use, whereas markerless monocular video still suffers from noise, missed detections, foreshortening, and perspective scale variation. **Aim of the article.** The aim is to develop and evaluate a reproducible markerless workflow that converts heterogeneous golf-stick video into interpretable kinematic indicators with explicit comparison of raw, filtered, and smoothed trajectories. **Objectives.** Objectives are to formalize filtering and smoothing; stabilize dynamic pixel-to-metre scaling; export path-quality and phase indicators; and quantify between-session dispersion while reporting diagnostic sensitivity, ablation, and keyframe-timing checks. **Methods.** The implemented pipeline uses offline MediaPipe-based landmarks, median pre-filtering, a constant-velocity Kalman filter with residual-adaptive measurement noise and physical gating, Rauch–Tung–Striebel smoothing, despiking with bounded polynomial smoothing, and dynamic scale calibration from the detected stick length with an assumed physical reference length. Apparent two-dimensional speed, acceleration, jerk, curvature, path efficiency, tempo, phase durations, and a smoothness index are exported. Evaluation covered all available heterogeneous field sessions under the scientific filtering profile. **Scientific novelty.** Novelty lies in coordinating these components in one reproducible workflow with transparent stage comparison and a clear split between implemented processing and planned external validation. **Practical significance.** Ordinary smartphone video can yield interpretable swing-quality indicators for research, coaching, and virtual-reality training without motion-capture hardware, if values are treated as apparent monocular two-dimensional estimates rather than laboratory ground truth. **Results.** All sessions were processed successfully. Smoothness index and path efficiency had the lowest between-session coefficients of variation, while peak derivative and phase metrics were highly dispersed. Keyframe-timing errors were large and are not accepted as accuracy evidence; sensitivity and ablation outputs remain computational diagnostics only. **Conclusions.** Global path-quality metrics are comparatively less dispersed than peak derivatives under heterogeneous capture, but measurement validity is unconfirmed until paired test–retest designs and independent spatial references are available.

**Keywords:** Markerless tracking; golf swing; Kalman filtering; trajectory smoothing; path efficiency; between-session dispersion

***For citation:*** **Syniuk I. M., Maksymov M. V., Maksymov O. M., Iyer Karthik "Markerless video-based golf-stick motion analysis using Kalman filtering and Rauch-Tung-Striebel smoothing". *Applied Aspects of Information Technology.* 2026; Vol.9 No.4: 512–526. DOI: https://doi.org/10.15276/aait.09.2026.33**

## INTRODUCTION

Quantitative assessment of human movement is important for sport biomechanics, rehabilitation, coaching technologies, and virtual-reality training systems. Traditional marker-based optical motion-capture systems can provide high spatial accuracy, but their practical use requires calibrated laboratory space, several synchronized cameras, reflective markers, trained operators, and post-processing procedures [1], [2]. These requirements limit repeated field use and reduce ecological validity in sports where natural motion and rapid setup are important.

Markerless computer-vision methods reduce this barrier by estimating human body landmarks and object landmarks from ordinary video [3], [4], [5]. For golf-stick movement, such a system can track the stick tip, estimate speed and angular motion, detect swing phases, and calculate movement-quality indicators. This is relevant for virtual-reality environments because the same measurement pipeline can support feedback, session comparison, and training analytics without specialized motion-capture hardware.

However, markerless tracking does not automatically produce reliable biomechanical measurements. Raw landmark coordinates from monocular video are affected by frame-to-frame

© Syniuk I., Maksymov M., Maksymov O., Iyer Karthik, 2026

This is an open access article under the CC BY license (http://creativecommons.org/licenses/by/4.0/deed.en)

noise, missed detections, outliers caused by motion blur or occlusion, and apparent scale changes caused by camera geometry. Differentiation amplifies these errors when velocity, acceleration, jerk, and angular velocity are computed [6], [7]. Therefore, a scientific article must not only show a visually plausible trajectory. It must explain the motion-processing pipeline, define the filtering and smoothing models, compare raw and processed signals, and report which metrics are stable enough for interpretation.

The present study develops a reproducible video-based pipeline for golf-stick motion analysis. The main contribution is not a new isolated filter, but a coordinated measurement workflow that combines robust landmark handling, Kalman filtering, backward smoothing, scale adaptation, phase segmentation, and between-session dispersion assessment on heterogeneous field video. This formulation addresses practical limitations of markerless recordings and frames the present outputs as diagnostic evidence pending controlled external validation. The overall processing architecture is shown in Fig. 1.

## LITERATURE REVIEW AND PROBLEM STATEMENT

Sports biomechanics has long used kinematic analysis to describe movement timing, segment coordination, implement speed, and movement smoothness [1], [2], [8]. In golf, relevant indicators include club or stick speed, swing tempo, wrist mechanics, shoulder and hip rotation, sequencing, and impact timing [9], [10], [11], [23]. Marker-based approaches remain the most controlled measurement option, while wearable inertial sensors provide a portable alternative for field instrumentation [24]; nevertheless, both are less convenient than ordinary video for rapid, routine field use.

Deep learning-based pose-estimation systems such as OpenPose and MediaPipe have made markerless analysis more practical [3], [4], [5]. These systems are widely used because they operate with ordinary cameras and can provide body landmarks in near real time [25], [29], [31]. Nevertheless, the accuracy and stability of markerless landmarks depend on camera view, lighting, motion blur, occlusion, and model confidence. Studies of motion-capture accuracy emphasize that sport applications require careful validation and that two-dimensional monocular projections cannot fully replace calibrated three-dimensional systems [12], [13], [26], [27], [28], [31].

Signal filtering is therefore essential. Median filtering is useful for suppressing impulse outliers [14]. Kalman filtering provides a recursive state estimate by combining a dynamic model with noisy measurements [15], [16]. When offline analysis is possible, Rauch-Tung-Striebel smoothing improves state estimates by using future observations after the forward pass [17]. Polynomial smoothing, including Savitzky-Golay-type approaches, can reduce derivative noise while preserving local trajectory shape [18]. In movement analysis, smoothness metrics based on jerk are commonly used but must be interpreted carefully because derivatives amplify measurement noise [19].

For markerless video-based golf-stick tracking, the unresolved problem is not only filtering the trajectory. A publication-quality method must also: (1) describe how landmarks and scale are obtained; (2) define how missing or uncertain measurements affect the filter; (3) compare raw, filtered, and smoothed trajectories; (4) quantify between-session dispersion on heterogeneous corpora without overclaiming test–retest repeatability; and (5) define external validation and sensitivity-analysis procedures. Without these elements, the study demonstrates software robustness but not yet full measurement validity.

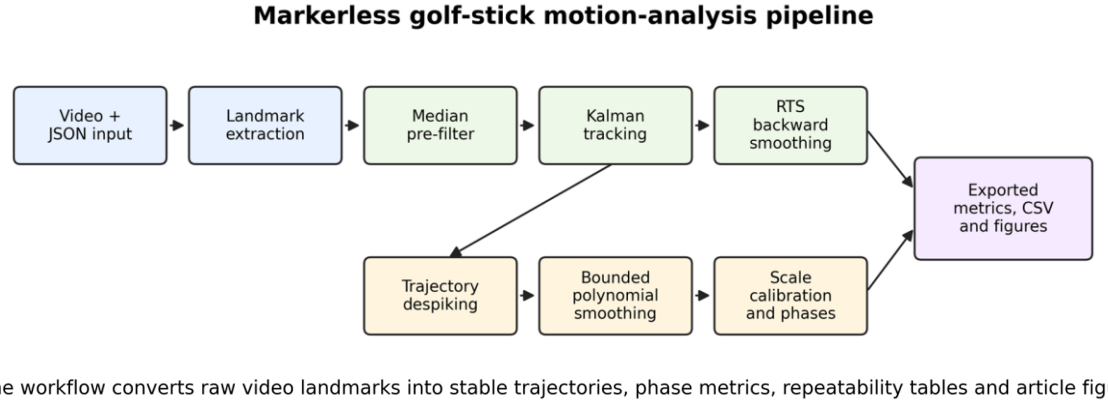



*Fig. 1.* **Architecture of the markerless golf-stick motion-analysis pipeline**
***Source:*** **compiled by the authors**

The problem addressed in this article is therefore the development and evaluation of a reproducible markerless pipeline that can process heterogeneous golf-stick videos, export scientifically interpretable metrics, and identify which indicators are stable enough for cross-session comparison.

## RESEARCH AIM AND OBJECTIVES

The aim of the research is to develop and evaluate a reproducible markerless video-based workflow for golf-stick motion analysis in sport-biomechanics and virtual-reality training applications.

The research objectives are:

1. To describe the complete motion-tracking pipeline from video landmarks to exported kinematic and biomechanical metrics.
2. To formulate the Kalman filtering and Rauch-Tung-Striebel smoothing stages used to stabilize the golf-stick tip trajectory.
3. To define raw, filtered, and smoothed trajectory streams and the comparison methodology between them.
4. To stabilize dynamic pixel-to-metre scaling under heterogeneous camera geometry.
5. To compute path-efficiency, curvature, smoothness, and phase-specific indicators.
6. To quantify between-session dispersion of exported metrics across the available processed sessions.
7. To report diagnostic keyframe-timing, controlled sensitivity perturbations, and ablation consistency checks, while clearly separating these diagnostics from planned controlled validation against independent spatial references.

## MATERIALS AND METHODS

### *Dataset and study design*

The present dataset contains recorded golf-stick swing sessions processed by the proposed markerless video-analysis pipeline. The evaluation export includes 71 processed sessions, all analysed with the scientific filtering profile. The recordings are heterogeneous in frame count and frame rate: the observed frame-rate range is 23.98-60.00 frames per second, and the frame count ranges from 60 to 1161 frames per session. Viewpoints, stroke categories, and quality tags are summarized in Table 1. This heterogeneity reflects practical field data but also increases variability of derivative and phase metrics. The parameters of the scientific filtering profile are listed in Table 2.

The dataset description reports the fields available in the processed exports. Approximately 15 athletes contributed recordings, but athlete identity and repeated-trial grouping are not encoded in the anonymized export; inclusion was limited to sessions that contained a complete preprocessed landmark file (mediapipe_data_full.json) and a processed video suitable for offline analysis. Therefore the between-session statistics reported in the Results section describe between-session dispersion across heterogeneous captures rather than within-athlete test–retest reliability or classical measurement repeatability. Session-level variability can reflect measurement uncertainty together with real differences in performers, swing type, viewpoint, and video quality.

*Table 1.* **Dataset reporting fields**

| Field | Value |
|---|---|
| Number of athletes | approximately 15 athletes (exact identity not encoded in the anonymized session export; session-level statistics are reported) |
| Number of processed sessions | 71 |
| Repetitions per athlete | not encoded in the anonymized session export; within-athlete test-retest analysis requires grouping metadata |
| Frame-rate range | 23.98-60.00 frames per second |
| Frame-count range | 60-1161 frames |
| Camera resolution classes | 480 × 706 to 1920 × 1080 pixels; detailed values are provided in the dataset-summary export |
| Recording viewpoint | 59 down-the-line sessions, 10 face-on sessions, two sessions without encoded view metadata |
| Stroke type | driver, wood, and iron categories appear in metadata; detailed values are provided in the dataset-summary export |
| Video-quality classes | metadata include slow-motion, super-slow-motion, motion-blur, and occlusion tags; detailed values are provided in the dataset-summary export |

***Source:*** **compiled by the authors**

*Table 2.* **Implemented scientific filtering profile and planned extensions**

| **Parameter** | **Scientific-profile value** |
|---|---|
| Landmark source | Offline MediaPipe 1.0.1 JSON (mediapipe_data_full.json) |
| STICK_REAL_LENGTH_M ($L_{ref}$) | 1.0 m |
| MEDIAN_WIN | 5 frames |
| STICK_CAL_WIN | 15 frames |
| Scale relative step clamp | 0.03 |
| Scale EMA $\alpha$ | 0.20 |
| Kalman $q_{pos}$, $q_{vel}$, $r_{meas}$ | 8.0, 8.0, 6.0 (defaults) |
| KF_MAX_MEAS_SPEED_PX_S | 2600 |
| KF_MAX_MEAS_ACCEL_PX_S2 | 38000 |
| KF_ADAPTIVE_RESIDUAL_PX | 10.0 |
| KF_ADAPTIVE_R_MULT_MAX | 9.0 |
| MAX_KF_PREDICT_GAP | 2 frames |
| TRAJ_DESPIKE_THRESH_PX / passes | 16.0 / 2 |
| TRAJ_POST_DESPIKE_THRESH_PX / passes | 9.0 / 1 |
| TRAJ_POLY_WIN / DEG | 7 / 2 |
| TRAJ_BLEND_RAW | 0.34 |
| TRAJ_MAX_DEV_PX | 9.0 |
| TRAJ_LAPLACE_PASSES / $\alpha$ | 3 / 0.45 |
| Native confidence-weighted $R_k$ | Not applied in reported runs |
| Controlled MoCap validation | Not completed in this article |

***Source:*** **compiled by the authors from the processing configuration**

### *Landmark extraction*

Each frame contains body landmarks and golf-stick landmarks obtained from an offline preprocessing stage that exports MediaPipe-based landmark JSON for every session (mediapipe_data_full.json), using the latest MediaPipe Python package available at dataset preparation (MediaPipe 1.0.1). The present article evaluates the downstream scientific filtering profile applied to those precomputed landmarks; training or re-implementation of the detector itself is outside the scope of this study. Normalized landmark coordinates are converted into pixel coordinates as:

$$p_k = (x_{\text{norm},k} \cdot W,\ y_{\text{norm},k} \cdot H),$$

where $W$ and $H$ are the frame width and height.
The main tracked object is the golf-stick tip. Stick base and middle points are used for orientation and scale estimation. Body landmarks are used in the software to calculate shoulder angle, hip angle, X-factor, wrist angle, and arc radius; these body-segment indicators are exported per frame but are reserved for future analysis and are not among the session-level metrics reported in this article.

The pipeline separates four trajectory streams, and the landmark configuration used for body and golf-stick tracking is illustrated in Fig. 2:

- raw trajectory obtained directly from detected landmarks;
- median-pre-filtered trajectory after local outlier suppression;
- Kalman-filtered trajectory after forward recursive estimation;
- smoothed trajectory after backward smoothing, despiking, and bounded polynomial smoothing.




*Fig. 2.* **Example frame with detected body and golf-stick landmarks**
***Source:*** **compiled by the authors**

### *Median pre-filtering*

A running median filter is applied independently to the horizontal and vertical stick-tip coordinates:

$$z_k^{\text{med}} = \text{median}(z_{k-m+1}, \ldots, z_k).$$

The median filter suppresses isolated one-frame landmark spikes without assuming Gaussian error distribution. This is important because markerless detections often contain impulse-like errors caused by occlusion or motion blur.

***Kalman filter formulation***

The forward filter uses a constant-velocity model for two-dimensional stick-tip tracking.

The state vector is:

$$x_k = [p_{x,k}, p_{y,k}, v_{x,k}, v_{y,k}]^T.$$

For inter-frame interval $\Delta t_k$, the transition matrix is:

$$F_k = [[1, 0, \Delta t_k, 0], [0, 1, 0, \Delta t_k], [0, 0, 1, 0], [0, 0, 0, 1]].$$

Only position is observed:

$$z_k = H\, x_k + \varepsilon_k, \quad H = [[1, 0, 0, 0], [0, 1, 0, 0]].$$

The prediction stage is:

$$\hat{x}_{k|k-1} = F_k\, \hat{x}_{k-1|k-1}$$
$$P_{k|k-1} = F_k\, P_{k-1|k-1}\, F_k^T + Q.$$

The update stage is:

$$y_k = z_k - H\, \hat{x}_{k|k-1}$$
$$S_k = H\, P_{k|k-1}\, H^T + R_k$$
$$K_k = P_{k|k-1}\, H^T\, S_k^{-1}$$
$$\hat{x}_{k|k} = \hat{x}_{k|k-1} + K_k\, y_k$$
$$P_{k|k} = (I - K_k\, H)\, P_{k|k-1}.$$

When a landmark is absent, only the prediction step is performed. This allows the filter to bridge short gaps without replacing missing measurements with artificial observations.

***Confidence-weighted measurement uncertainty***

In the implemented scientific profile, measurement noise is adapted from the innovation residual magnitude (residual-adaptive $R$), which down-weights physically implausible or unstable updates. A detector-confidence form can additionally be written as:

$$R_k = (r_0 / \max(c_k, c_{\min}))\, I_2 \quad \text{(optional confidence form)},$$

where $r_0$ is baseline measurement variance and $c_{\min}$ prevents numerical instability. Native per-landmark detector confidence was not uniformly available in the present export; therefore the confidence-weighted $R_k$ form is retained as an optional extension, whereas the residual-adaptive schedule and physical gates described above are the implemented uncertainty controls used for all reported results.

***Outlier gating***

Outlier rejection is performed using physical plausibility and innovation checks. A standard innovation-distance criterion is:

$$d_k^2 = y_k^T\, S_k^{-1}\, y_k.$$

Measurements exceeding a threshold are rejected or down-weighted. Additional gates include maximum frame-to-frame displacement, plausible stick length, and landmark availability. These gates reduce derivative artifacts caused by single-frame tracking errors.

***Rauch-Tung-Striebel smoothing***

For offline scientific analysis, the forward Kalman estimates are refined using the Rauch-Tung-Striebel smoother. The backward gain is:

$$G_k = P_{k|k}\, F_k^T\, P_{k+1|k}^{-1}.$$

The smoothed state is:

$$\hat{x}_k^T = \hat{x}_{k|k} + G_k\, (\hat{x}_{k+1}^T - F_k\, \hat{x}_{k|k}).$$

The smoothed covariance is:

$$P_k^T = P_{k|k} + G_k\, (P_{k+1}^T - P_{k+1|k})\, G_k^T.$$

The forward Kalman output is suitable for lower-latency feedback. The RTS-smoothed output is used for offline analysis because it uses later observations to refine earlier estimates.

***Trajectory despiking and bounded polynomial smoothing***

After RTS smoothing, local trajectory spikes are corrected using neighbouring trajectory structure. A bounded local polynomial smoother is then applied so that the final trajectory reduces derivative noise without drifting excessively from the observed path. This step is necessary because even smoothed position estimates can produce unstable acceleration and jerk if residual local artifacts remain.

***Dynamic scale calibration***

The pixel-to-metre conversion uses the detected stick length in the image plane. Because a monocular 2D projection mixes camera distance with foreshortening when the stick rotates out of plane, the resulting quantities are apparent image-plane metric estimates under an assumed physical stick length, not fully calibrated three-dimensional biomechanical measurements.

The detected length is:

$$L_k^{\text{px}} = \|p_k^{\text{tip}} - p_k^{\text{base}}\|_2.$$

The scale factor is:

$$s_k = L_{\text{ref}} / \text{median}(L_{k-w+1}^{\text{px}}, \ldots, L_k^{\text{px}}) \quad [\text{m/pixel}],$$

with units metres per pixel. In code and in all reported speeds, metric displacement is obtained by multiplying pixel displacement by $s_k$ (not by dividing by $s_k$). The scale is bounded (maximum relative step 0.03) and exponentially smoothed ($\alpha$ = 0.20) to reduce jumps caused by viewpoint change, partial occlusion, and apparent stick-length variation. Without a calibrated plane, homography, multi-camera geometry, or independent length measurement, absolute metre values remain model-dependent apparent 2D estimates.

***Kinematic and phase metrics***

For smoothed position $p_k$ (pixels), time interval $\Delta t_k$, and scale $s_k$ (m/pixel), apparent linear speed is:

$$v_k = (\|p_k - p_{k-1}\|_2 / \Delta t_k) \cdot s_k \quad [\text{m/s}].$$

Acceleration and jerk are:

$$a_k = (v_k - v_{k-1}) / \Delta t_k,$$
$$j_k = (a_k - a_{k-1}) / \Delta t_k.$$

Stick angle is:

$$\theta_k = \text{atan2}(p_{y,k}^{\text{tip}} - p_{y,k}^{\text{base}}, p_{x,k}^{\text{tip}} - p_{x,k}^{\text{base}}),$$
$$\omega_k = \text{wrap}(\theta_k - \theta_{k-1}) / \Delta t_k.$$

Path efficiency is:

$$E_k^{\text{path}} = \|p_k - p_0\|_2 / \Sigma_{i=1}^{k} \|p_i - p_{i-1}\|_2.$$

Local curvature is computed from the triangle formed by three consecutive trajectory points:

$$\kappa_k = 4 A_k / (a \cdot b \cdot c),$$

where $A_k$ is triangle area and $a$, $b$, and $c$ are side lengths.

The smoothness index (SI) reported in this study is defined as SI = $-\log_{10}$ (mean ($j_k^2$)), i.e. the negative base-ten logarithm of the mean squared jerk of the smoothed trajectory; a lower mean squared jerk yields a larger (less negative) index. Because the mean squared jerk of the scaled trajectories exceeds unity, the resulting index values are negative. Path efficiency is the ratio of net displacement to path length along the trajectory (Equation below).

The swing is divided into backswing and downswing phases. If ball detection is available, impact is detected by stick-tip-to-ball proximity; otherwise, maximum speed is used as a proxy. Phase indicators include backswing duration, downswing duration, swing tempo, backswing peak speed, and downswing peak speed.

***Raw, filtered and smoothed comparison***

The pointwise deviation between the final smoothed trajectory and the raw trajectory is:

$$e_k = \|p_k^{\text{smooth}} - p_k^{\text{raw}}\|_2.$$

The comparison reports mean median, percentile deviation, maximum deviation, root-mean-square jerk, and threshold exceedance counts. This comparison measures how strongly the pipeline regularizes the raw trajectory. It does not replace external accuracy validation because raw landmarks are not a ground truth.

***Validation and reliability protocols***

To complement the between-session dispersion statistics, the study reports three diagnostic blocks that are already implemented on the present corpus: an external keyframe-timing comparison against available annotations, sensitivity perturbations (frame thinning, simulated landmark dropout, and scale perturbation), and an ablation consistency check across processing variants. A controlled reference-validation subset is planned for future work and should additionally include dense manual annotation of impact, top of backswing, start of downswing, and several control points along the stick-tip trajectory, ideally with an independent spatial reference (calibrated plane, multi-camera reconstruction, or motion capture). Accuracy should then be reported as event-timing error, geometric trajectory error, absolute and relative scalar error, and correlation or concordance with reference values.

Sensitivity analysis includes frame thinning, simulated landmark dropout, and scale perturbation at the dose levels reported in the Results section. The ablation check compares median-only, Kalman-only, Kalman plus RTS, and the full pipeline on the same 71-session corpus; derivative-based ablation metrics are treated as diagnostic because units, time normalization, and residual spikes can differ sharply between variants (see Discussion). Classical test–retest reliability (within-subject SD/CV, ICC, and Bland–Altman limits) requires repeated measures of the same athletes under a fixed protocol and is therefore listed as future work rather than a completed result [20], [21], [22].

Between-session dispersion is summarized using the coefficient of variation and a dispersion coefficient analogous in form to the classical repeatability coefficient, but interpreted here only as a between-session spread measure on a heterogeneous corpus:

$$\text{CV} = (\text{SD} / |\bar{x}|) \times 100\ \%,$$

$RC_{disp} = 1.96 \cdot \sqrt{2} \cdot SD \approx 2.77 \cdot SD$ (between session dispersion).

For paired repeated measurements, Bland-Altman limits of agreement are:

$LoA = \bar{d} \pm 1.96\ SD_d$ (for future paired repeated measures).

## RESEARCH RESULTS

### *Processing completion*

The scientific filtering profile processed all 71 discovered sessions successfully. No failed sessions were reported in the evaluation export. The completion summary is given in Table 3.

### Between-session dispersion

Between-session dispersion statistics were computed for 11 exported metrics. The smoothness index had the lowest coefficient of variation among reported indicators, followed by path efficiency; within this corpus they are therefore the comparatively least dispersed indicators, not proven test-retest reliable measures. Maximum speed and downswing peak speed had identical summary values in the available exports, indicating that maximum speed occurred during the downswing in the processed sessions. Higher-order derivative and phase metrics showed substantially larger dispersion. The ranking is summarized in Table 4 and Fig. 3.

*Table 3.* **Processing completion**

| Indicator | Value |
|---|---|
| Total discovered sessions | 71 |
| Successfully processed sessions | 71 |
| Failed sessions | 0 |
| Completion rate | 100 % |
| Filtering profile | scientific |

***Source:*** **compiled by the authors**

*Table 4.* **Between-session dispersion statistics across processed sessions**

| Metric | Mean | SD | CV, % | $RC_{disp}$ | Interpretation |
|---|---|---|---|---|---|
| Smoothness index | -5.882 | 1.266 | 21.52 | 3.508 | least dispersed in this corpus |
| Path efficiency | 0.726 | 0.277 | 38.17 | 0.769 | comparatively low dispersion |
| Maximum speed, m/s | 8.184 | 9.681 | 118.28 | 26.833 | affected by session heterogeneity |
| Downswing peak speed, m/s | 8.184 | 9.681 | 118.28 | 26.833 | same as maximum speed in current exports |
| Swing tempo | 0.604 | 0.777 | 128.63 | 2.154 | sensitive to phase detection |
| Curvature RMS | 1063.382 | 1686.764 | 158.62 | 4675.470 | sensitive to local geometry |
| Downswing duration, s | 1.676 | 2.812 | 167.72 | 7.793 | heterogeneous timing |
| Maximum angular velocity, rad/s | 10.169 | 19.601 | 192.76 | 54.331 | derivative-sensitive |
| Maximum acceleration, m/s² | 185.158 | 400.392 | 216.24 | 1109.831 | exploratory under heterogeneous capture |
| Backswing duration, s | 0.673 | 1.517 | 225.35 | 4.206 | sensitive to phase definition |
| Backswing peak speed, m/s | 1.065 | 5.533 | 519.31 | 15.337 | least stable reported metric |

***Source:*** **compiled by the authors**

*Note. CV denotes the coefficient of variation,* $CV = (SD/|mean|) \times 100\ \%$. *RC denotes a between-session dispersion coefficient computed as* $RC = 1.96 \cdot \sqrt{2} \cdot SD \approx 2.77 \cdot SD$*; it is reported for comparability with common reporting practice but is not a classical within-subject repeatability coefficient, because athlete identity and repeated trials are not encoded. Maximum speed and downswing peak speed share identical statistics because the peak stick-tip speed occurred during the downswing in all processed sessions (expected coincidence, not a typesetting error)*

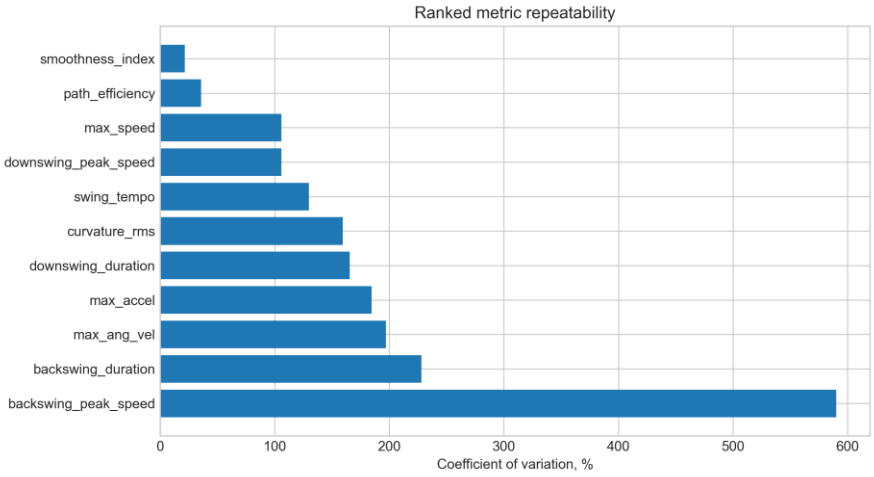



*Fig. 3.* **Ranked between-session dispersion of exported swing metrics by coefficient of variation**
***Source:*** **compiled by the authors**

***Raw-versus-smoothed trajectory deviation***

A representative exported trajectory was evaluated by comparing raw and final exported stick-tip positions (Table 5; Fig. 4). This analysis quantifies the deviation introduced by filtering and smoothing, but it is not an external accuracy test.

***Reference validation, sensitivity and ablation results***

External keyframe diagnostics (Table 6; Fig. 5), sensitivity-analysis results (Table 7; Fig. 6), and ablation consistency results (Table 8; Fig. 7) are summarized below.

*Table 5.* **Raw-versus-smoothed trajectory deviation for representative exported swing**

| Indicator | Value |
|---|---|
| Valid samples | 141 |
| Mean deviation, m | 0.053 |
| Median deviation, m | 0.050 |
| 90-th percentile deviation, m | 0.063 |
| 95-th percentile deviation, m | 0.067 |
| 99-th percentile deviation, m | 0.069 |
| Maximum deviation, m | 0.139 |
| RMS jerk | 1446.560 |
| Frames with deviation above 3 cm | 141 |
| Frames with deviation above 5 cm | 51 |

***Source:*** **compiled by the authors**

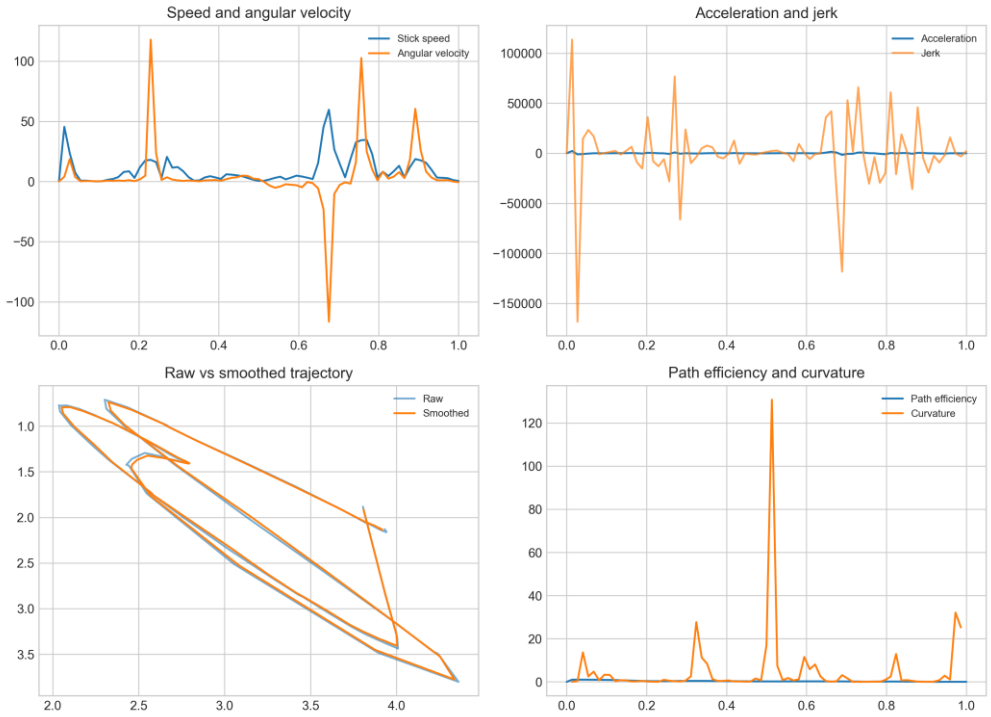



*Fig. 4.* **Example kinematic plots and raw-versus-smoothed stick-tip trajectory**
***Source:*** **compiled by the authors**

These blocks are interpreted as diagnostic evidence from the present heterogeneous dataset, not as final controlled validation against a laboratory motion-capture system and not as proof of measurement efficacy. The reference-validation table compares automatic event timing with available keyframe annotations; because not every session contains all reference events, the number of available reference pairs differs by event.

*Table 6.* **Reference keyframe timing diagnostic**

| Validation target | Metric | Diagnostic result and interpretation |
|---|---|---|
| Impact timing | mean absolute error, frames and ms | 118.79 frames; 2694.21 ms; n = 20; large mismatch, not accepted as final accuracy evidence |
| Top of backswing timing | mean absolute error, frames and ms | 194.25 frames; 4933.33 ms; n = 8; large mismatch, not accepted as final accuracy evidence |
| Start of downswing timing | mean absolute error, frames and ms | 152.15 frames; 3872.28 ms; n = 20; large mismatch, not accepted as final accuracy evidence |
| Stick-tip control points | mean geometric error | not computed in the present diagnostic export; requires point-level manual reference extraction |
| Scalar metrics | absolute and relative error | not computed in the present diagnostic export; requires independent reference scalar metrics |
| Scalar metrics | correlation or concordance | not computed in the present diagnostic export; requires independent reference scalar metrics |

***Source:*** **compiled by the authors from the keyframe-diagnostic export**

*Table 7.* **Sensitivity-analysis results**

| Perturbation | Primary reporting metric | Result |
|---|---|---|
| Frame thinning | median absolute percentage change | smoothness 13.03 %; path efficiency 8.66 %; maximum speed 36.45 %; curvature RMS 69.08 %; swing tempo 61.45 % |
| Landmark dropout | median absolute percentage change | smoothness 15.10 %; path efficiency 13.42 %; maximum speed 29.94 %; curvature RMS 22.10 %; swing tempo 61.71 % |
| Scale perturbation | median absolute percentage change | smoothness 0.70 %; path efficiency 0.00 %; maximum speed 5.00 %; curvature RMS 4.76 %; swing tempo 0.00 % |
| Combined degradation | retained or changed stable-metric classification | not computed in the present diagnostic export; retained for future controlled-degradation testing |

***Source:*** **compiled by the authors from the sensitivity-analysis export**

*Table 8.* **Paired ablation consistency diagnostic (same 71 sessions; shared derivatives and time base)**

| Pipeline variant | Completion rate | Mean trajectory deviation, m | RMS jerk (paired) | Smoothness index (paired) |
|---|---|---|---|---|
| Median only | 71/71 | 0.153 | 14448.5 | -8.320 |
| Kalman without RTS | 71/71 | 0.094 | 881.0 | -5.890 |
| Kalman plus RTS without despiking | 71/71 | 1.414 | 180.9 | -4.515 |
| Full pipeline | 71/71 | 0.019 | 11835.4 | -8.146 |

***Source:*** **compiled by the authors from the re-run paired ablation export**

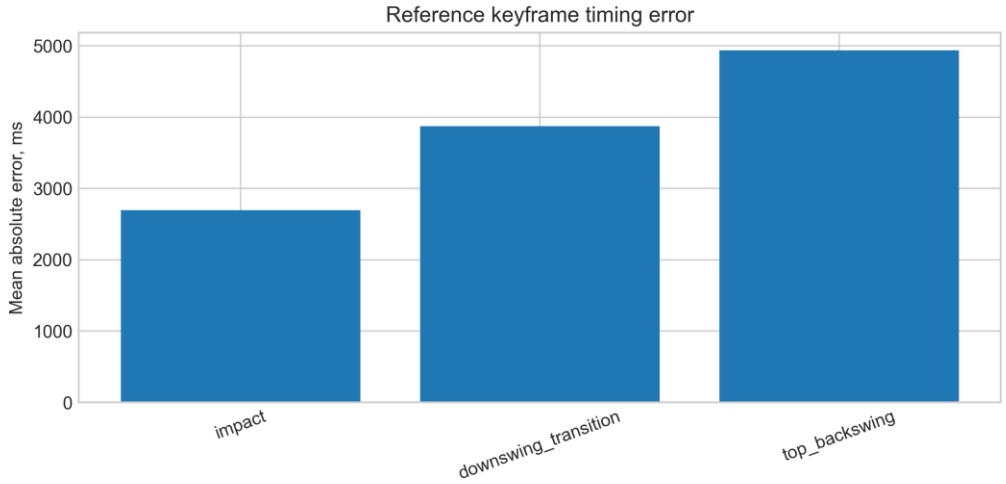



*Fig. 5.* **Mean absolute timing error between automatic events and reference keyframes**
***Source:*** **compiled by the authors**

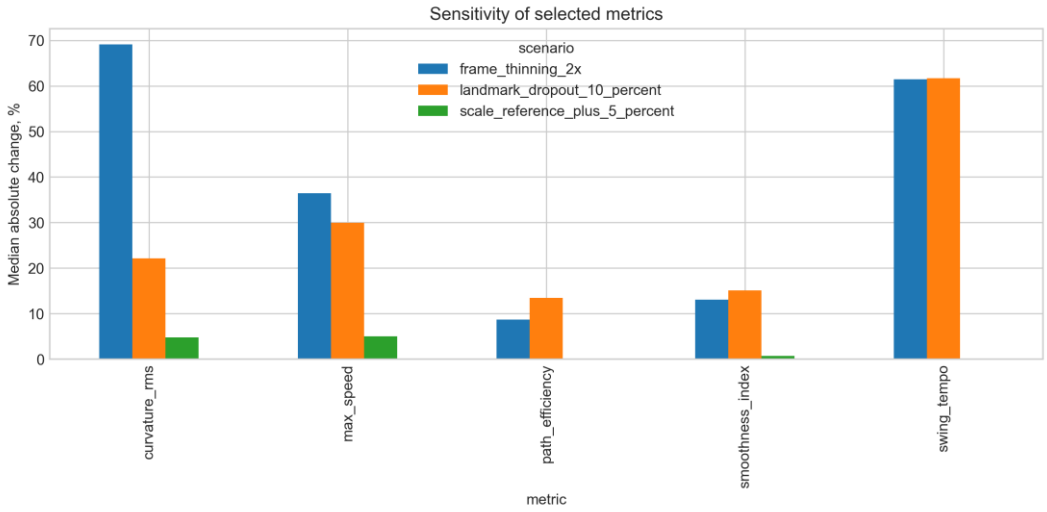



*Fig. 6.* **Sensitivity of selected metrics under controlled input perturbations**
***Source:*** **compiled by the authors**

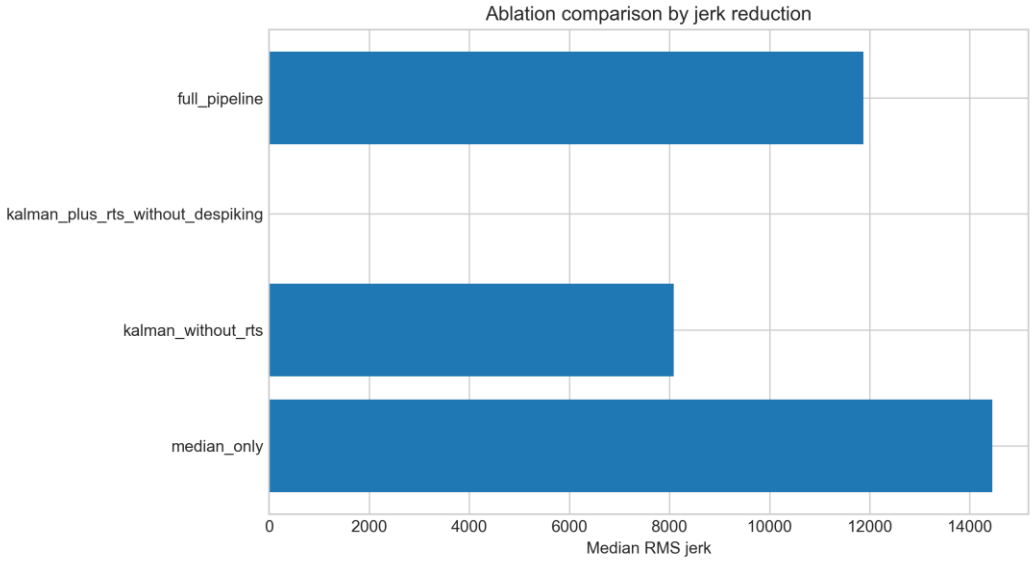



*Fig. 7.* **Ablation comparison of trajectory-processing variants**
***Source:*** **compiled by the authors**

The keyframe timing errors in Table 6 (about 2.7-4.9 s) are larger than the temporal scale of a typical golf swing and are therefore treated as evidence that automatic event mapping requires recalibration before accuracy claims. Processing of 71/71 files demonstrates software completeness, not measurement accuracy. Table 8 reports a re-run paired ablation on the same 71 sessions with one derivative definition and one time base. Mean trajectory deviation is lowest for the full pipeline (0.019 m), while RTS stages strongly reduce RMS jerk relative to median-only processing; the full pipeline again shows higher RMS jerk because later blending reintroduces high-frequency components toward the raw landmarks. These values are stage-consistency diagnostics, not external accuracy proof.

## DISCUSSION OF RESULTS

The completed results show that the proposed workflow is operationally robust for the available dataset: all processed sessions were completed with the scientific profile. The between-session dispersion ranking is more informative than a single visual example because it shows which metrics remain comparatively less dispersed across heterogeneous recordings. It does not, however, establish classical repeatability or external accuracy.

On the present heterogeneous dataset, smoothness index and path efficiency emerged as the comparatively least dispersed indicators. These indicators summarize global trajectory quality and are less dependent on one isolated frame. By contrast, maximum acceleration, maximum angular velocity, backswing peak speed, curvature RMS, and phase-duration metrics showed high dispersion and should be interpreted as exploratory unless recording conditions and phase segmentation are controlled [30].

The raw-versus-smoothed trajectory comparison shows that the final trajectory is meaningfully regularized. The average deviation between raw and final exported trajectories indicates that the pipeline does not merely reproduce raw landmarks. At the same time, this result must not be misinterpreted as external accuracy. A smoothed signal can be more biomechanically useful than a raw signal, but a reference annotation is required to determine whether it is more correct.

The methodological value of the pipeline lies in the coordinated use of several components. Median filtering reduces isolated spikes; Kalman filtering provides a physically interpretable state estimate; confidence-weighted measurement noise offers a formal uncertainty model; gating reduces implausible updates; RTS smoothing improves offline trajectories; despiking and bounded polynomial smoothing reduce residual artifacts; and dynamic calibration controls scale instability.

The main limitation is that the current reference validation is based only on available event keyframes and not on dense point-level manual trajectories or independent scalar reference metrics. Dynamic stick-length scaling cannot separate camera distance from out-of-plane foreshortening; therefore reported metre-based speeds and accelerations are apparent 2D plane estimates. The next empirical step is to annotate stick-tip control points and reference scalar metrics for a representative subset of sessions and, where possible, to add a calibrated plane, multi-view geometry, or motion-capture reference. Sensitivity analysis and ablation have been added as batch outputs, but they should be interpreted as computational robustness tests rather than a substitute for independent laboratory validation. Finally, because the system is monocular and two-dimensional, out-of-plane motion and perspective distortion remain unresolved limitations.

## CONCLUSIONS

The study presents a reproducible markerless video-based workflow for golf-stick motion analysis in virtual-reality and sport-biomechanics applications. The workflow combines landmark extraction, median pre-filtering, Kalman tracking, Rauch–Tung–Striebel smoothing, trajectory despiking, bounded polynomial smoothing, dynamic scale calibration, phase segmentation, and between-session dispersion assessment.

The completed evaluation shows that all available sessions were processed successfully and that global movement-quality metrics are less dispersed than peak derivative metrics under heterogeneous recording conditions. On the present corpus, smoothness index and path efficiency are therefore the most defensible candidates for exploratory cross-session comparison, whereas maximum acceleration and angular-velocity peaks should be treated as exploratory. Practical measurement efficacy remains unconfirmed until controlled external validation and within-subject reliability studies are completed.

The scientific novelty consists in the coordinated integration of known filtering and smoothing tools into a reproducible golf-stick measurement workflow with explicit trajectory-stage comparison and cautious between-session interpretation. The practical value is the possibility

of extracting interpretable apparent 2D movement indicators from ordinary video for coaching feedback and VR training analysis. Future work must complete reference validation against independent spatial standards, paired sensitivity and ablation experiments, and formal agreement statistics.

## ACKNOWLEDGMENTS

The authors thank the research supervisor and collaborators who supported the review of the manuscript and the development of the motion-analysis workflow.

**Conflicts of Interest:** The authors declare that there is no conflict of interest regarding this study, including financial, personal, authorship, or other interests that could influence the research and its results presented in this article

**Funding:** This research was conducted without external financial support

**Data availability:** Aggregate tables and diagnostic summaries supporting the findings are reported in this article. The processing source code and project materials are available in the public repository https://github.com/ivansinuyk/vr_motion. Raw video recordings and full per-frame trajectory archives are not reproduced in the manuscript because of privacy and file-size constraints; they are available from the corresponding author upon reasonable request for research reuse

**Use of generative AI tools:** AI-assisted language revision, consistency checking, and manuscript editing were performed with Claude Fable, GPT Astra, and GPT-5.6 Sol / Composer in Cursor during preparation of this revised version (2026). The authors remain responsible for all data, methods, interpretation, references, and final text; all AI-assisted fragments were checked and edited by the authors. AI was not used to fabricate results, formulas, or references

## REFERENCES

1. Winter, D. A. “Biomechanics and motor control of human movement”. *4th ed. Hoboken, NJ, USA: Wiley*. 2009. DOI: https://doi.org/10.1002/9780470549148.

2. Payton, C. J. & Burden, A. (Eds.). “Biomechanical evaluation of movement in sport and exercise: The British Association of Sport and Exercise Sciences Guide*”. 2nd ed. Abingdon, UK: Routledge*. 2018. DOI: https://doi.org/10.4324/9781315776871.

3. Cao, Z., Hidalgo, G., Simon, T., Wei, S. E. & Sheikh, Y. “OpenPose: Realtime multi-person 2D pose estimation using part affinity fields”. *IEEE Transactions on Pattern Analysis and Machine Intelligence.* 2021; 43 (1): 172–186, https://www.scopus.com/record/display.uri?eid=2-s2.0-85070219994. DOI: https://doi.org/10.1109/TPAMI.2019.2929257.

4. Bazarevsky, V., Grishchenko, I., Raveendran, K., Zhu, T., Zhang, F. & Grundmann, M. “BlazePose: On-device real-time body pose tracking”. *Proceedings of the CVPR Workshop on Computer Vision for Augmented and Virtual Reality.* Seattle, WA, USA. 2020. DOI: https://doi.org/10.48550/arXiv.2006.10204.

5. Lugaresi, C., Tang, J., Nash, H., McClanahan, C., Uboweja, E., Hays, M., Zhang, F., Chang, C. L., Yong, M. G., Lee, J., Chang, W. T., Hua, W., Georg, M. & Grundmann, M. “MediaPipe: A framework for building perception pipelines”. *arXiv preprint.* 2019. DOI: https://doi.org/10.48550/arXiv.1906.08172.

6. Camomilla, V., Cereatti, A., Cutti, A. G., Fantozzi, S., Stagni, R. & Vannozzi, G. “Methodological factors affecting joint moments estimation in clinical gait analysis: a systematic review”. *BioMedical Engineering OnLine*. 2017; 16: 106. DOI: https://doi.org/10.1186/s12938-017-0396-x.

7. Pagnon, D., Domagnan, M. & Reveret, L. “Pose2Sim: an end-to-end workflow for 3D markerless sports kinematics from consumer-grade cameras”. *Sports Biomechanics*. 2022. DOI: https://doi.org/10.1080/14763141.2022.2110618.

8. Bourgain, M., Hybois, S., Thoreux, P., Rouillon, O., Rouch, P. & Sauret, C. “Effect of shoulder model complexity on kinematics and kinetics of the golf swing”. *Sports Biomechanics*. 2022. DOI: https://doi.org/10.1080/14763141.2022.2130433.

9. Evans, K. & Tuttle, N. “Improving performance of golfers with a coaching and biomechanics feedback intervention: a single-subject design”. *Sports Biomechanics*. 2020. DOI: https://doi.org/10.1080/14763141.2018.1556329.

10. Sim, T., Choi, A., Lee, S. & Mun, J. H. “Markerless motion capture estimates of lower extremity kinematics and kinetics in golfers”. *Sensors*. 2022; 22 (4): 1554. DOI: https://doi.org/10.3390/s22041554.

11. Joyce, C. “The most important “factor” in producing clubhead speed in golf”. *Human Movement Science.* 2017; 55: 138–144. DOI: https://doi.org/10.1016/j.humov.2017.08.003.

12. van der Kruk, E. & Reijne, M. M. “Accuracy of human motion capture systems for sport applications: state-of-the-art review”. *European Journal of Sport Science*. 2018; 18 (6): 806–819, https://www.scopus.com/record/display.uri?eid=2-s2.0-85045751825.
DOI: https://doi.org/10.1080/17461391.2018.1463397.

13. Ota, M., Tateuchi, H., Hashiguchi, T. & Ichihashi, N. “Verification of reliability and validity of motion analysis systems during bilateral squat using human pose tracking algorithm”. *Gait & Posture*. 2020; 80: 62–67, https://www.scopus.com/record/display.uri?eid=2-s2.0-85085754655.
DOI: https://doi.org/10.1016/j.gaitpost.2020.05.027.

14. Sinclair, J., Edmundson, C. J., Brooks, D. & Hobbs, S. J. “Evaluation of kinematic methods of identifying gait events during running at different speeds”. *Journal of Biomechanics*. 2018. DOI: https://doi.org/10.1016/j.jbiomech.2018.05.006.

15. Kalman, R. E. “A new approach to linear filtering and prediction problems”. *Journal of Basic Engineering*. 1960; 82 (1): 35–45. DOI: https://doi.org/10.1115/1.3662552.

16. Welch, G. & Bishop, G. “An introduction to the Kalman filter”. *Technical Report TR 95-041. Chapel Hill, NC, USA: University of North Carolina at Chapel Hill*, 2006. – Available from: https://www.cs.unc.edu/~welch/media/pdf/kalman_intro.pdf. – [Accessed: Apr. 29, 2026].

17. Rauch, H. E., Tung, F. & Striebel, C. T. “Maximum likelihood estimates of linear dynamic systems”. *AIAA Journal*. 1965; 3 (8): 1445–1450, https://www.scopus.com/record/display.uri?eid=2-s2.0-84945697750. DOI: https://doi.org/10.2514/3.3166.

18. Savitzky, A. & Golay, M. J. E. “Smoothing and differentiation of data by simplified least squares procedures”. *Analytical Chemistry*. 1964; 36 (8): 1627–1639, https://www.scopus.com/record/display.uri?eid=2-s2.0-33947453419. DOI: https://doi.org/10.1021/ac60214a047.

19. Balasubramanian, S., Melendez-Calderon, A., Roby-Brami, A. & Burdet, E. “On the analysis of movement smoothness”. *Journal of NeuroEngineering and Rehabilitation.* 2015; 12: 112, https://www.scopus.com/record/display.uri?eid=2-s2.0-84953214858. DOI: https://doi.org/10.1186/s12984-015-0090-9.

20. Impellizzeri, F. M. & Marcora, S. M. “Test–retest reliability of physiological parameters in sport science: a practical guide”. *International Journal of Sports Physiology and Performance*. 2019. DOI: https://doi.org/10.1123/ijspp.2018-0614.

21. Koo, T. K. & Li, M. Y. “A guideline of selecting and reporting intraclass correlation coefficients for reliability research”. *Journal of Chiropractic Medicine.* 2016; 15 (2): 155–163. https://www.scopus.com/record/display.uri?eid=2-s2.0-84963540533.
DOI: https://doi.org/10.1016/j.jcm.2016.02.012.

22. Bland, J. M. & Altman, D. G. “Statistical methods for assessing agreement between two methods of clinical measurement”. *The Lancet.* 1986; 327 (8476): 307–310, https://www.scopus.com/record/display.uri?eid=2-s2.0-0022571143. DOI: https://doi.org/10.1016/S0140-6736(86)90837-8.

23. Mo, S. & Chow, D. H. K. “Segmental sequencing in golf swing and its relation to clubhead speed”. *Sports Biomechanics.* 2018; 17 (3): 429–441, https://www.scopus.com/record/display.uri?eid=2-s2.0-85029525987. DOI: https://doi.org/10.1080/14763141.2017.1371213.

24. Camomilla, V., Bergamini, E., Fantozzi, S. & Vannozzi, G. “Trends supporting the in-field use of wearable inertial sensors for sport performance evaluation: a systematic review”. *Sensors*. 2018; 18 (3): 873. DOI: https://doi.org/10.3390/s18030873.

25. Colyer, S. L., Evans, M., Cosker, D. P. & Salo, A. I. T. “A review of the evolution of vision-based motion analysis and the integration of advanced computer vision methods towards developing a markerless system”. *Sports Medicine – Open.* 2018; 4: 24, https://www.scopus.com/record/display.uri?eid=2-s2.0-85048302366. DOI: https://doi.org/10.1186/s40798-018-0139-y.

26. Wade, L., Needham, L., McGuigan, P. & Bilzon, J. “Applications and limitations of current markerless motion capture methods for clinical gait biomechanics”. *PeerJ*. 2022; 10: e12995, https://www.scopus.com/record/display.uri?eid=2-s2.0-85125709321.
DOI: https://doi.org/10.7717/peerj.12995.

27. Needham, L., Evans, M., Cosker, D. P., Wade, L., McGuigan, P. M., Bilzon, J. L. & Colyer, S. L. “The accuracy of several pose estimation methods for 3D joint centre localisation”. *Scientific Reports.* 2021; 11 (1): 20673. https://www.scopus.com/record/display.uri?eid=2-s2.0-85117132097.
DOI: https://doi.org/10.1038/s41598-021-00212-x.

28. Stenum, J., Rossi, C. & Roemmich, R. T. “Two-dimensional video-based analysis of human gait using pose estimation”. *PLOS Computational Biology*. 2021; 17 (4): e1008935,. https://www.scopus.com/record/display.uri?eid=2-s2.0-85104998893. DOI: https://doi.org/10.1371/journal.pcbi.1008935.

29. Cust, E. E., Sweeting, A. J., Ball, K. & Robertson, S. “Machine and deep learning for sport-specific movement recognition: a systematic review of model development and performance”. *Journal of Sports Sciences*. 2019; 37 (5): 568–600, https://www.scopus.com/record/display.uri?eid=2-s2.0-85053196097. DOI: https://doi.org/10.1080/02640414.2018.1521769.

30. Sweeting, A. J., Cormack, S. J., Morgan, S. & Aughey, R. J. “When is a sprint a sprint? A review of the analysis of team-sport athlete activity profile”. *Frontiers in Physiology*. 2017; 8: 432, https://www.scopus.com/record/display.uri?eid=2-s2.0-85021858935.
DOI: https://doi.org/10.3389/fphys.2017.00432.

31. Nakano, N., Sakura, T., Ueda, K., Omura, L., Kimura, A., Iino, Y., Fukashiro, S. & Yoshioka, S. “Evaluation of 3D markerless motion capture accuracy using OpenPose with multiple video cameras”. *Frontiers in Sports and Active Living*. 2020; 2: 50. DOI: https://doi.org/10.3389/fspor.2020.00050.

Received 23.07.2026
Received after revision 11.09.2026
Accepted 24.09.2026

**DOI: https://doi.org/10.15276/hait.09.2026.33**
**УДК 004.932:004.94:796.352**

# Безмаркерний відеоаналіз руху ключки для гольфу з використанням фільтрації Калмана та згладжування Рауха-Тунга-Штрібеля

**Синюк Іван Миколайович[1)]**
ORCID: https://orcid.org/0009-0000-4141-0135; i.syniuk@gmail.com
**Максимов Максим Віталійович[1)]**
ORCID: https://orcid.org/0000-0002-7536-2570; prof.maksimov@gmail.com. Scopus Author ID: 7005088554
**Максимов Олексій Максимович[1)]**
ORCID: https://orcid.org/0000-0003-2504-0853; oleksii.maksymov@op.edu.ua. Scopus Author ID: 57220057510
**Айєр Картік[2)]**
ORCID: https://orcid.org/0009-0003-2520-1810; ki2406@columbia.edu
[1)] Національний університет «Одеська політехніка», просп. Шевченка, 1. Одеса, 65044, Україна
[2)] Колумбійський університет, 116-та вулиця та Бродвей. Нью-Йорк, 10027, США

## АНОТАЦІЯ

**Актуальність.** Кількісне оцінювання руху ключки для гольфу важливе для спортивної біомеханіки, тренування, реабілітації та систем віртуальної реальності. Лабораторне маркерне захоплення руху точне, але незручне у полі, а безмаркерне монокулярне відео містить шум, пропуски, скорочення проєкції та перспективні зміни масштабу, тому сирі орієнтири не є каліброваними біомеханічними вимірюваннями. **Метою статті** є розробка та оцінювання відтворюваного безмаркерного пайплайну, що перетворює гетерогенне відео на інтерпретовані кінематичні показники з порівнянням сирих, фільтрованих і згладжених траєкторій. **Завдання.** Формалізувати фільтрацію та згладжування; стабілізувати динамічне масштабування; експортувати показники якості траєкторії та фаз; оцінити міжсесійну дисперсію й навести діагностики чутливості, абляції та хронометражу ключових кадрів. **Методи.** Реалізований пайплайн використовує офлайн MediaPipe-орієнтири, медіанну передфільтрацію, фільтр Калмана з адаптивним за залишком шумом вимірювань і фізичним ґейтингом, згладжування Рауха–Тунга–Штрібеля, усунення викидів з обмеженим поліноміальним згладжуванням та динамічну калібрацію масштабу за виявленою довжиною ключки із заданою еталонною довжиною. Експортуються видимі двовимірні оцінки швидкості, прискорення, ривка, кривизни, ефективності траєкторії, темпу, тривалостей фаз та індексу плавності. Оцінювання виконано на всіх доступних гетерогенних сесіях за науковим профілем фільтрації. **Наукова новизна.** Новизна — скоординована інтеграція компонентів у відтворюваний процес із прозорим поетапним порівнянням і розмежуванням реалізованих і запланованих блоків валідації. **Практична значимість.** Звичайне відео зі смартфона дає інтерпретовані показники якості свінгу для досліджень, тренерського зворотного зв’язку та тренувань у віртуальній реальності без систем захоплення руху, якщо величини трактуються як видимі монокулярні двовимірні оцінки. **Результати.** Усі сесії опрацьовано успішно. Індекс плавності та ефективність траєкторії мали найнижчі міжсесійні коефіцієнти варіації, тоді як пікові похідні та фазові метрики були сильно розсіяні. Похибки ключових кадрів великі й не приймаються як доказ точності; чутливість і абляція – лише обчислювальні діагностики. **Висновки.** Глобальні показники якості траєкторії порівняно менш розсіяні за

пікові похідні, проте вимірювальна валідність непідтверджена до парних test–retest протоколів і незалежних просторових еталонів; подальша робота має завершити еталонну валідацію та формальну статистику узгодженості.

**Ключові слова:** безмаркерне відстеження; гольф-свінг; фільтрація Калмана; згладжування траєкторії; ефективність траєкторії; міжсесійна дисперсія

## ABOUT THE AUTHORS



**Ivan M. Syniuk** - PhD student, Department of Computer Intelligent Systems and Networks. Odesa Polytechnic National University, 1, Shevchenko Ave. Odesa, 65044, Ukraine
ORCID: https://orcid.org/0009-0000-4141-0135; i.syniuk@gmail.com
***Research field:*** markerless motion analysis; computer vision; Kalman filtering and trajectory smoothing; sport biomechanics; virtual-reality training systems

**Синюк Іван Миколайович** – аспірант кафедри Комп'ютерних інтелектуальних систем і мереж. Національний університет «Одеська політехніка», просп. Шевченка, 1. Одеса, 65044, Україна.
***Галузь досліджень:*** безмаркерний аналіз рухів; комп'ютерний зір; фільтрація Калмана та згладжування траєкторій; спортивна біомеханіка; системи тренування у віртуальній реальності



**Maksym V. Maksymov** - Doctor of Engineering Sciences, Professor, Head of Department of Computer Intelligent Systems and Networks. Odesa Polytechnic National University, 1, Shevchenko Ave. Odesa, 65044, Ukraine
ORCID: https://orcid.org/0000-0002-7536-2570; prof.maksimov@gmail.com; Scopus Author ID: 7005088554
***Research field:*** automation and control systems; intelligent measurement systems; data analysis and processing; computer modelling of complex technical objects; decision-support systems

**Максимов Максим Віталійович** – доктор технічних наук, професор, завідувач кафедри Комп'ютерних інтелектуальних систем і мереж. Національний університет «Одеська політехніка», просп. Шевченка, 1. Одеса, 65044, Україна
***Галузь досліджень:*** автоматизовані системи управління; інтелектуальні вимірювальні системи; аналіз і обробка даних; комп'ютерне моделювання складних технічних об'єктів; системи підтримки прийняття рішень



**Oleksii M. Maksymov** - PhD in Engineering, Associate Professor, Department of Computer Intelligent Systems and Networks. Odesa Polytechnic National University, 1, Shevchenko Ave. Odesa, 65044, Ukraine
ORCID: https://orcid.org/0000-0003-2504-0853; oleksii.maksymov@op.edu.ua; Scopus Author ID: 57220057510
***Research field:*** computer vision; digital signal and image processing; intelligent information systems; software engineering; applied machine learning
**Максимов Олексій Максимович** – кандидат технічних наук, доцент кафедри Комп'ютерних інтелектуальних систем і мереж. Національний університет «Одеська політехніка», просп. Шевченка, 1. Одеса, 65044, Україна
***Галузь досліджень:*** комп'ютерний зір; цифрова обробка сигналів і зображень; інтелектуальні інформаційні системи; програмна інженерія; прикладне машинне навчання



**Karthik Iyer** - Researcher. Columbia University, 116th Street and Broadway. New York, NY 10027, USA
ORCID: https://orcid.org/0009-0003-2520-1810; ki2406@columbia.edu
***Research field:*** computer vision; applied machine learning; biomedical engineering; image-based motion measurement; sport and rehabilitation technologies

**Айєр Картік** – дослідник. Колумбійський університет, 116-та вулиця та Бродвей. Нью-Йорк, 10027, США.
***Галузь досліджень:*** комп'ютерний зір; прикладне машинне навчання; біомедична інженерія; вимірювання рухів на основі зображень; спортивні та реабілітаційні технології